American Mineralogist, Volume 84, pages 782–789, 1999

Chemical and paragenetic data on gadolinite-group minerals from Baveno and Cuasso al Monte, southern Alps, Italy

F. PEZZOTTA,[1,*] V. DIELLA,[2] AND A. GUASTONI[1]

[1]Museo Civico di Storia Naturale, Corso Venezia 55, 20121 Milan, Italy
[2]National Research Council, Centro di Studio per la Geodinamica alpina e quaternaria, Via Botticelli 23, 20133 Milan, Italy

ABSTRACT

A chemical and paragenetic study was performed on gadolinite-group minerals occurring in miarolitic pink granite and granophyric leucogranite of the subvolcanic Hercynian plutons at Baveno and Cuasso al Monte, Southern Alps, Italy. In the localities investigated, gadolinite-group minerals are hosted in massive pegmatite, in aplite, and in miarolitic cavities having different degrees of evolution. The petrological relations indicate that progressive crystallization has occurred from magmatic through to hydrothermal conditions. At Baveno, Ce-rich gadolinite-(Y) (with ΣREE >Y) formed during the primitive stages of pegmatite crystallization. Gadolinite-(Y) (with ΣREE <Y) formed in pegmatites and granophyric aplites during primitive to moderately evolved stages of these dikes. Gadolinite-(Y) (with ΣREE <Y) and hingganite-(Y), which contains a significant amount of the datolite component, occur in miarolitic cavities together with several rare-element accessory phases. During the latest stages, datolite formed with zeolites. At Cuasso al Monte, gadolinite is found only in primitive to highly evolved miarolitic cavities. The cores of these crystals consist of Nd-rich gadolinite-(Y) (with ΣREE >Y). Gadolinite-(Y) (with ΣREE <Y) formed during intermediate stages of evolution, and hingganite-(Y) is dominant in highly evolved miarolitic cavities together with several rare-element phases. The chemical differences observed in the gadolinites from the two localities may indicate a different parental magma composition and reflect a difference in the crystallization processes. In contrast to Baveno, the crystallization at Cuasso al Monte occurred under open-system conditions, which prevented the formation of a zeolite (datolite-bearing) stage and generated a typical medium- to low-temperature hydrothermal mineral assemblage consisting of quartz, fluorite, barite, sulfides, and carbonates. The large variations in the Y/Dy ratio observed in the studied samples may be due to a change in the fluorine abundance in hydrothermal fluids related to paragenetic effects and mixing processes.

INTRODUCTION

Some minerals of the gadolinite group [gadolinite-(Y), gadolinite-(Ce), hingganite-(Y), hingganite-(Yb), hingganite-(Ce), and minasgeraisite] are typical of Nb-Y-F-rich pegmatites (NYF-pegmatites, Černý 1991) and alkaline pegmatites throughout the world. Examples include: Ytterby, Sweden (Mason 1971); Oslo Region, Norway (Larsen 1996); Khibina Massif in the Kola Peninsula, Russia (Khomyakov 1995; Belolipetskii and Voloshin 1996); Sichuan, China (Wu et al. 1996); and Minas Gerais, Brazil (Foord et al. 1986).

In the granite plutons of Baveno and Cuasso al Monte (Southern Alps, NW Italy), several gadolinite-group minerals have been reported (Grill 1937; Fagnani 1941; Pagliani 1941; Boscardin et al. 1970; Gramaccioli 1975; Kipfer 1983). These authors described the gadolinites from Baveno as "isotropic" (metamict) crystals hosted by feldspar in the pegmatitic veins and those from miarolitic cavities in the pink Baveno granite and the Cuasso al Monte granophyre as euhedral fresh or altered crystals.

This work reports paragenetic and chemical data obtained on gadolinite-group minerals found in the miarolitic NYF-pegmatites, the granite, and the granophyre of both the Baveno and Cuasso al Monte localities. These minerals are recognized in pegmatitic systems as crystallizing from primitive magmatic conditions through to highly evolved hydrothermal conditions, which show extensive changes in their compositions, particularly during the latest stages of evolution of the miarolitic cavities. Our results show that the gadolinite-group minerals may be of petrological interest in the characterization of the pegmatitic, pneumatolitic, and hydrothermal stages of granite plutons.

GEOLOGIC SETTING

The western part of the South Alpine basement contains several granitic intrusions and rhyolite flows of Permian age (Fig. 1), which comprise a late- to post-orogenic, K-rich magmatic province. These effusives and intrusives were emplaced as either rhyolitic ignimbrites or pink subsolvus granites at subvolcanic levels (Bonin 1988). In particular, the Baveno pluton, with an age of 277 ± 8 Ma (Rb-Sr whole-rock isochrons; Pinarelli et al. 1988), contains large quantities of a pink miarolitic facies rich in fluorite, zinnwaldite, zeolites, and

*E-mail: federico@r10.terra.unimi.it

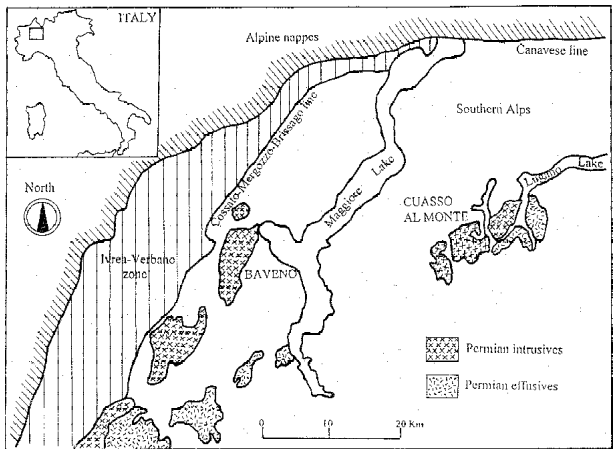

FIGURE 1. Geological sketch map of the western portion of the Southern Alps including the Hercynian plutonic and volcanic rocks.

magnetite-fayalite nodules (Boriani et al. 1992). The abundance of pegmatitic cavities and miarolitic aplitic-pegmatitic dikes, and the presence of a large granophyric dike in the upper part of the intrusion indicate subvolcanic crystallization conditions.

At Cuasso al Monte, a Permian caldera structure was identified by Bakos et al. (1990). In this caldera, a thick sequence of volcanic rocks was intruded by a leucogranitic pluton (275 ± 8 Ma, Rb-Sr whole rock isochron; Bakos et al. 1990) mainly composed of aplitic microgranite and miarolitic granite having a granophyric texture. Aplitic-pegmatitic pods and veins, locally related to large miarolitic cavities, are widespread. Circulation of abundant late hydrothermal fluids was responsible for the crystallization of many different minerals in the cavities, local alteration of feldspars, and chloritization of biotite in the granite.

MINERALOGY AND PARAGENESIS OF THE MIAROLITIC CAVITIES

The parageneses of Baveno and Cuasso al Monte, reported in Figures 2 and 3, have been deduced from field studies and from observations in thousands of specimens in private and public collections (Museo di Storia Naturale of Milan).

In the Baveno pluton, miarolitic cavities occur isolated in the pink facies of the granite, in pegmatitic veins (where they have irregular shapes), and in aplitic-pegmatitic dikes. These dikes contain granophyric portions characterized by several small cavities in the aplitic units, and large, vertically elongated, cavities in the pegmatitic units. These cavities range from 1 cm up to 2–3 m in diameter. All the cavities developed as isolated systems and, in some cases, the largest ones underwent a partial collapse. The paragenesis (Fig. 2) is typical of NYF-pegmatites and developed under magmatic, pneumatolitic, and hydrothermal conditions. Among the Y-REE minerals, only the gadolinite group is present from the earliest magmatic stage to the latest low-temperature hydrothermal event. In particular, at low temperature, datolite crystallized together with zeolites. The chemical complexity of the fluids that were present in these pockets is revealed by the presence of, in addition to F-rich minerals (fluorite, topaz, and zinnwaldite), Be-silicates,

BAVENO

Fluid saturation in magma	Pneumatolitic conditions	HT-MT hydrothermal conditions	LT hydrothermal conditions
Quartz			
Feldspars			
Fayalite			
Siderophyllite			
Gadolinite group[1]			
Zircon			
Be-silicates[2]			
Zinnwaldite and muscovite			
Cassiterite			
Y-REE silicates[3]			
Fe,Ti, U oxides[4]			
Topaz			
Xenotime-(Y)			
Sulphides[5]			
Fluorite			
Wolframates and molybdates[6]			
Aeschynite (series)			
Sc-silicates[7]			
Babingtonite			
Schorl			
Phosphates[8]			
Titanite and Fe-axinite			
Clinochlore, epidote and pumpellyite-(Fe^{+2})			
Calcio-ancylite-(Nd)			
Carbonates and sulfates[9]			
Zeolites[10], opal and prehnite			
Chrysocolla			

[1] Gadolinite-(Y), gadolinite-(Ce), hingganite-(Y) and datolite; [2] bavenite, bertrandite, beryl and gugiaite; [3] allanite and kainosite-(Y); [4] anatase, hematite, magnetite, rutile and uraninite; [5] arsenopyrite, chalcopyrite, galena, molybdenite and pyrite; [6] scheelite, and wulfenite; [7] bazzite, cascandite, jervisite, scandiobabingtonite and thortveitite; [8] apatite group minerals, herderite and hydroxylherderite; [9] calcite, malachite and barite; [10] chabazite, heulandite, ltumontite and stilbite. Minerals not sufficiently characterized have not been included in the list.

Scandiobabingtonite after P. Orlandi (personal communication); other minerals after Guastoni and Pezzotta (in press), and references therein.

FIGURE 2. Paragenetic sequence observed in the miarolitic cavities of the Baveno pluton.

CUASSO AL MONTE

Fluid saturation in magma	Pneumatolitic conditions	HT-MT hydrothermal conditions	LT hydrothermal conditions
Quartz			
Feldspars			
Fayalite			
Siderophyllite			
Zinnwaldite and muscovite			
Zircon			
Y-REE silicates[1]			
Gadolinite group[2]			
Y-REE phosphates[3]			
Topaz			
Sulphides[4]			
Fluorite			
Aeschynites (series)			
Schorl			
Fe,Ti, Cu oxides[5]			
Lollingite			
Phosphates[6]			
Sc-silicates[7]			
Be-silicates[8]			
Titanite			
Y-REE carbonates[9]			
Clinochlore and epidote			
Carbonates and sulfates[10]			
Silver			
Arsenates and molybdates[11]			
Opal, hemimorphite and pirophyllite			
Todorokite and Mn-oxides			

[1] Allanite and kainosite-(Y); [2] gadolinite-(Y), Nd rich gadolinite and hingganite-(Y); [3] monazite-(Ce) and xenotime-(Y); [4] arsenopyrite, chalcopyrite, galena, marcasite, molybdenite, pyrite, sphalerite and stibnite; [5] anatase, brookite, cuprite and hematite; [6] apatite group and herderite; [7] bazzite and thortveitite; [8] bertrandite and phenakite; [9] bastnasite (series) and synchysite (series); [10] ankerite, calcite, cerussite, dolomite, malachite, siderite and barite; [11] adamite, agardite-(Y), pharmacosiderite, powellite and wulfenite. Minerals reported in literature but not sufficiently characterized have not been included in the list.

Bazzite, cuprite, powellite and thortveitite after I. Campostrini, P. Gentile, E. Sinelli and P. Vignola (personal communications); other minerals after Guastoni and Pezzotta (in press), and references therein.

FIGURE 3. Paragenetic sequence observed in the cavities of the Cuasso al Monte granophyric granite.

Y-REE silicates, xenotime-(Y), aeschynite-group, calcio-ancylite-(Nd), Sc-silicates, and Fe-, Ti-, and U-oxides. Most of these minerals seem to have crystallized from hydrothermal fluids at high-*T* to medium-*T* conditions; at lower temperature, locally abundant zeolites with minor amounts of carbonates cover the previous minerals.

At Cuasso al Monte, miarolitic cavities (typically smaller than 1 cm) are abundant throughout the entire outcrop of the granophyric granite. Larger cavities (up to 1 or 2 m) have a

characteristic vertically elongated shape and are commonly rooted in an aplitic-pegmatitic pod or vein. Microtextural and structural observations indicate that most of these larger cavities were interconnected during their crystallization. In many cases carbonates, sulfates, and/or fluorite have filled the cavities completely during the latest stages of fluid circulation. Circulation of hydrothermal fluids under open-system conditions is indicated by the presence of crosscutting barite-fluorite-quartz-sulfides-arsenates veins.

The high-temperature paragenesis at Cuasso al Monte (Fig. 3) is similar to that at Baveno. At medium and low temperatures, a significant difference is observed between the two localities, which is due to the abundance of carbonates, fluorite, and sulfides, and the absence of zeolites in the cavities at Cuasso al Monte. Moreover, gadolinite-group minerals are not present in the early stages at Cuasso al Monte, in contrast to Baveno, nor has datolite been reported there.

SAMPLES INVESTIGATED

Eight samples of unaltered gadolinite-group minerals were carefully selected from different outcrops of the Baveno and Cuasso al Monte intrusions and prepared as polished sections. The samples were representative of the different parageneses observed in the intrusions and were considered of interest for detailed electron microprobe analyses. The main features of these samples are reported below (the sample numbers in the mineral collection of the Museo di Storia Naturale of Milan are indicated within parentheses). Micrographs of some of the samples are shown in Figure 4.

Sample B1 (M.13801) is a subhedral crystal hosted in coarse-grained quartz and feldspar from the massive primitive part of a pegmatitic dike in the Baveno pink granite. The crystal is 20 mm and black in color; it was collected at the beginning of this century, probably in the dumps of the old granite quarry close to the town of Baveno.

Sample B2 (M.13783) is a subhedral crystal hosted in the primitive medium-grained, massive portion of a pegmatitic dike intruded into the Baveno pink granite. The crystal is 12 mm and similar to sample B1; it was collected in the 1960s, close to the town of Baveno.

Sample B3 (M.29956) is a mass of subhedral crystals hosted in the granophyric portion of the aplitic unit of a zoned subhorizontal aplitic-pegmatitic dike from the upper part of the Baveno pluton. The crystals are 5–8 mm and black in color; they are locally altered into a reddish translucent material associated with Fe oxides.

Sample B4 (M.30271) is a subhedral crystal, 10 mm, found in a cavity where it grew from the surface of an albite crystal.

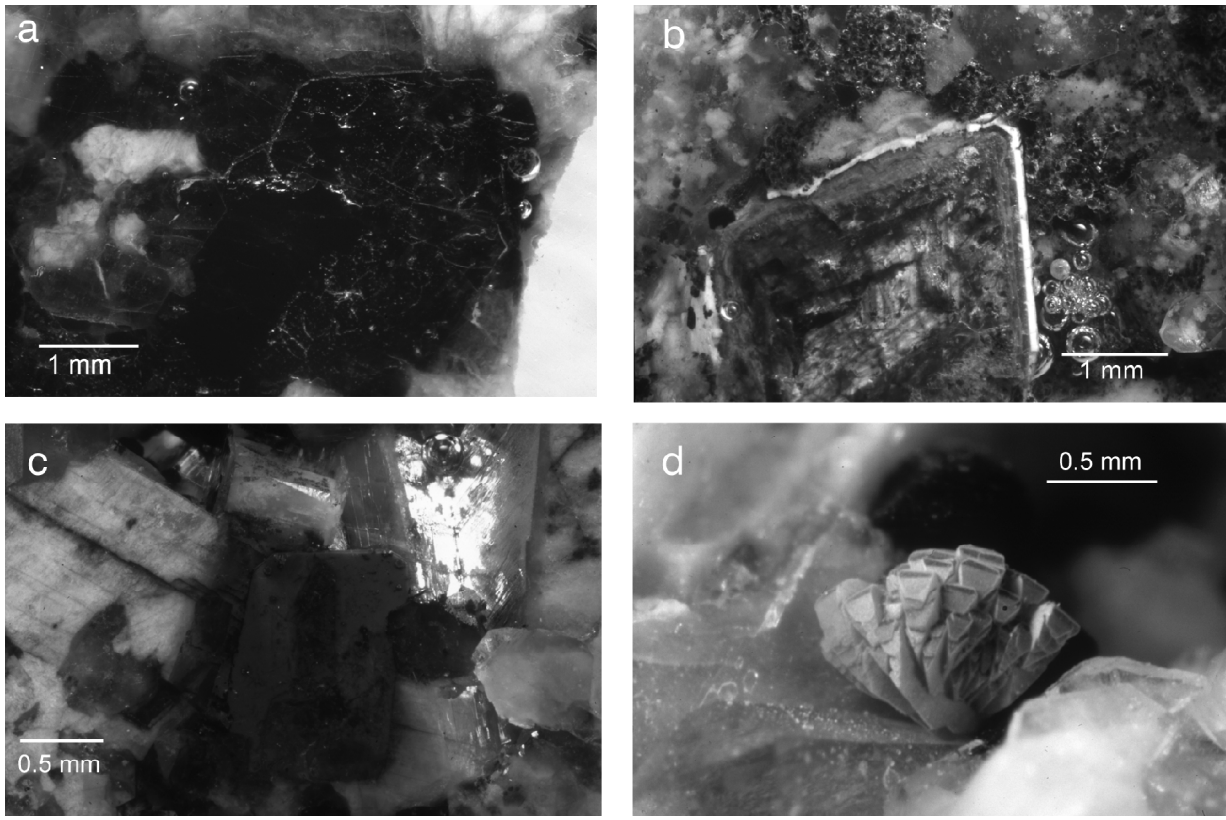

FIGURE 4. Photomicrographs of some of the studied samples: **(a)** sample B3, polished section, the gadolinite crystal (brown to black) is surrounded by gray quartz and pink feldspar; **(b)** sample B5, polished section, strongly zoned gadolinite crystal with a white overgrowth of hingganite composition; **(c)** sample C1, polished section, zoned gadolinite crystal surrounded by pink feldspar: darker small grains inside the crystal are marcasite inclusions; **(d)** group of well-formed gadolinite-hingganite crystals collected in the same cavity of sample C3.

The crystal is strongly zoned, with a brown-black core and a millimeter-sized white overgrowth. Associated minerals include fluorite, epidote, and zeolites. This sample was collected at the Oltrefiume quarry, close to the town of Baveno.

Sample B5 (M.30275) is an euhedral crystal, 4 mm, found in a cavity where it grew from the surface of quartz and feldspar, together with zinnwaldite, clinochlore, and fluorite. The crystal is zoned similarly to sample B4 and was collected in the Madre quarry, close to the town of Baveno.

Samples C1 (M.30272) and C2 (M 30273) are subhedral crystals, 2 mm, hosted in feldspar and found within a small cavity together with siderophyllite. The crystals are gray-brown in color and zoned internally, with a darker core containing abundant marcasite inclusions. The samples were collected in the granophyre of Cuasso al Monte in two different areas of the Bonomi quarry, close to Lugano Lake.

Sample C3 (M.30274) is a well-formed euhedral crystal, 1.5 mm, with a core rooted in feldspar on the wall of a small miarolitic cavity. In the cavity, the presence of fluorite, clinochlore, and Y-REE carbonates indicate a well-developed, low-temperature hydrothermal event. The crystal is strongly zoned, with a darker core and a translucent white rim. The sample was collected from the granophyre outcrop at the Laghetto quarry, close to the village of Cuasso al Monte.

ANALYTICAL METHODS

Chemical analyses and backscattered electron images were performed on polished samples using an Applied Research Laboratories electron microprobe fitted with six wavelength-dispersive spectrometers and a Tracor Northern energy dispersive spectrometer. The system was operated at an accelerating voltage of 20 kV, a sample current of 10 nA (on brass), and a counting time of 10 or 20 s on peak and 5 or 10 s on backgrounds. A series of natural (kaersutite for Ca, Si, Fe) and syn-

TABLE 1. Selected analyses of gadolinite group minerals from Baveno

	B1						B2	B3			B4	B5				
	σ%*	core	core	core	rim	rim	avg. 5 pts core/rim	core	avg. 4 pts inter	avg. 4 pts rim	core/ inter	rim	core	inter	inter	rim
wt%																
La_2O_3	0.6	1.7	1.6	2.2	1.7	1.5	0.4	0.9	1.0	1.0	1.3	0.7	1.3	1.1	1.2	0.4
Ce_2O_3	0.6	8.7	8.7	10.6	8.7	8.1	2.6	3.9	3.6	3.8	5.1	2.5	4.4	4.4	4.3	0.6
Pr_2O_3	0.8	1.4	1.3	1.8	1.6	1.4	0.6	1.3	1.1	1.2	1.3	1.0	1.0	1.1	1.1	0.5
Nd_2O_3	1.6	7.0	6.8	8.2	4.7	4.5	4.5	8.4	4.6	4.5	4.8	5.1	3.1	3.6	3.8	1.9
Sm_2O_3	1.4	3.7	3.8	4.1	3.2	2.4	3.3	3.9	3.3	3.4	3.3	3.8	2.5	2.5	2.3	2.3
Gd_2O_3	2.3	3.3	3.2	3.6	2.2	2.4	4.4	4.9	4.6	4.3	3.8	4.3	2.8	3.2	2.9	4.3
Dy_2O_3	2.5	2.9	2.7	2.9	2.5	2.5	3.8	3.7	3.5	3.1	3.5	2.8	3.2	2.6	2.1	3.7
Er_2O_3	2.8	2.1	1.9	2.1	2.3	2.2	2.1	2.3	1.8	1.8	2.1	2.1	1.9	1.8	1.8	2.4
Yb_2O_3	2.7	2.2	2.2	2.4	3.2	3.2	1.8	2.2	1.8	1.5	1.7	1.5	1.7	2.2	2.3	2.2
Y_2O_3	1.2	16.5	15.5	15.5	21.7	20.6	25.7	20.5	26.9	27.6	19.6	22.4	19.5	22.6	21.9	27.3
ThO_2	1.2	1.7	1.9	1.1	1.8	2.0	0.6	0.8	0.2	0.2	1.3	0.6	0.4	1.2	1.0	0.2
UO_2	0.3	0.6	0.6	0.6	0.9	0.7	0.2	0.2	0.3	0.2	0.4	<0.1	<0.1	0.5	0.6	0.2
CaO	0.4	0.8	0.7	0.4	0.8	0.8	0.4	2.3	0.5	0.7	3.2	4.1	5.1	3.8	5.8	6.8
FeO†	0.9	12.5	12.5	12.5	12.9	13.0	13.3	9.2	13.9	13.6	9.2	3.1	5.0	8.3	8.0	2.6
SiO_2	1.0	21.4	22.4	21.0	22.4	22.7	22.8	22.1	23.1	23.2	23.1	25.0	26.3	24.3	23.7	26.1
BeO‡		8.9	9.3	8.7	9.3	9.5	9.5	9.2	9.6	9.6	9.6	10.4	11.0	10.1		
H_2O‡		0.1	0.2	0.0	0.1	0.1	0.1	1.0	0.0	0.1	1.1	3.0	2.7	1.6		
Total		95.3	95.4	97.8	100.1	97.8	96.0	96.8	100.1	99.9	94.5	92.4	91.6	94.8		
Formula proportions based on 10 O atoms																
La		0.06	0.05	0.08	0.06	0.05	0.01	0.03	0.03	0.03	0.04	0.02	0.04	0.04	0.04	0.01
Ce		0.30	0.29	0.36	0.28	0.26	0.08	0.13	0.11	0.12	0.16	0.08	0.13	0.13	0.13	0.02
Pr		0.05	0.04	0.06	0.05	0.05	0.02	0.04	0.04	0.04	0.04	0.03	0.03	0.03	0.03	0.01
Nd		0.23	0.22	0.27	0.15	0.14	0.14	0.26	0.14	0.14	0.15	0.15	0.09	0.11	0.12	0.05
Sm		0.12	0.12	0.13	0.10	0.07	0.10	0.12	0.10	0.10	0.10	0.11	0.07	0.07	0.07	0.06
Gd		0.10	0.10	0.11	0.07	0.07	0.13	0.14	0.13	0.12	0.11	0.12	0.07	0.09	0.08	0.11
Dy		0.09	0.08	0.09	0.07	0.07	0.11	0.10	0.10	0.09	0.10	0.07	0.08	0.07	0.06	0.09
Er		0.06	0.05	0.06	0.06	0.06	0.06	0.06	0.05	0.05	0.06	0.05	0.05	0.05	0.05	0.06
Yb		0.06	0.06	0.07	0.09	0.09	0.05	0.06	0.05	0.04	0.04	0.04	0.04	0.06	0.06	0.05
Y		0.82	0.75	0.77	1.02	0.97	1.21	0.97	1.23	1.26	0.91	0.98	0.83	1.01	0.98	1.12
Th		0.04	0.04	0.02	0.04	0.04	0.01	0.02	0.00	0.00	0.03	0.01	0.01	0.02	0.02	0.00
U		0.01	0.01	0.01	0.02	0.01	0.00	0.00	0.01	0.00	0.01	0.00	0.00	0.01	0.01	0.00
Ca		0.08	0.07	0.04	0.08	0.08	0.04	0.22	0.05	0.07	0.30	0.36	0.44	0.34	0.53	0.57
Fe		0.98	0.95	0.98	0.95	0.97	0.98	0.68	1.00	0.98	0.67	0.21	0.33	0.58	0.56	0.16
Si		2.00	2.05	1.96	1.98	2.02	2.02	1.96	1.99	1.99	2.01	2.04	2.12	2.03	2.00	2.01
Be		2.00	2.05	1.96	1.98	2.02	2.02	1.96	1.99	1.99	2.01	2.04	2.12	2.03		
OH		0.04	0.15	0.01	0.07	0.09	0.05	0.60	0.01	0.03	0.67	1.62	1.45	0.88		
Me		2.0	1.9	2.1	2.1	2.0	2.0	2.2	2.0	2.1	2.1	2.0	1.9	2.0	2.2	2.2
Me/Si		1.0	0.9	1.1	1.0	1.0	1.0	1.1	1.0	1.0	1.0	1.0	0.9	1.0	1.1	1.1
Y/Dy		9.5	9.7	8.7	14.3	13.4	11.1	9.2	12.8	14.5	9.2	13.3	10.2	14.4	17.0	12.0
st.dev. of Y/Dy for averaged analysis						0.1		0.6	0.8							

* Percentage standard deviation based on counting statistics.
† Total iron as FeO.
‡ Calculated as explained in the text.

thetic standards (synthetic UO_2 for U and $LiBO_2$ glasses prepared as specified in Mannucci et al. 1986, for REE, Th, and Y) were employed. In all the samples examined here, the concentrations of F, Mg, Al, P, S, Sc, Mn, Sr, Ba, Tb, and Ho are below the limits of detection (~0.05 wt%). The results were corrected for matrix effects using a modified version of the MAGIC IV program, and the interferences among the REE were corrected as specified in Mannucci et al. (1986).

The X-ray powder-diffraction (XRD) analyses were performed using a Rigaku D/IIIMAX diffractometer using Ni-filtered Cu$K\alpha$ radiation and quartz as an internal standard.

RESULTS

Representative analyses for each sample from Baveno and Cuasso al Monte are shown in Tables 1 and 2, respectively. For crystals with a relatively homogeneous composition, an average of the analysed points is presented. The structural formulae were calculated based on 10 O atoms assuming the general formula $[W_{2-3}X(B,Be)_2(Si,B)_2(O,OH)_{10}]$, where W = Ca, Y, REE, U, Th; X = Y, Fe^{2+}, and Mg.

Boron and beryllium could not be detected by our microprobe. Therefore, the concentration of Be was calculated assuming that Be and Si occur in equal amounts. If the Ca was > 0.5 atoms per formula units (apfu), which indicates a considerable datolite or homilite component, then large amounts of B could substitute for Be; therefore, in such cases, we have not calculated the amount of Be (Tables 1 and 2). Iron was considered exclusively in the divalent state (see discussion in Demartin et al. 1993). Hydrogen atoms were introduced to compensate the charges due to the vacancies on the X-site.

The low totals in some of the analyses might be explained by a mineral alteration facilitated by the metamict state. Indeed, even if some exceptions occur, a rough negative correlation between totals and Th and U abundance can be observed.

TABLE 2. Selected analyses of gadolinite group minerals from Cuasso al Monte

	C1			C2						C3					
	σ%*	inter	rim	core	core	inter	core/ inter	inter/ rim	rim	core	core	inter	inter/ rim	rim	rim
(wt%)															
La_2O_3	0.6	0.9	0.9	0.9	1.0	1.0	1.0	1.0	0.6	1.2	1.3	1.3	1.5	1.3	1.0
Ce_2O_3	0.6	3.3	3.3	3.9	4.4	4.0	4.8	4.2	2.0	5.3	5.6	3.7	3.9	4.0	3.0
Pr_2O_3	0.8	1.0	1.1	1.4	1.4	1.2	1.6	1.3	0.8	1.7	1.6	0.9	0.9	1.1	0.9
Nd_2O_3	1.6	4.1	5.4	5.1	5.8	5.7	5.5	5.5	4.9	7.3	6.8	2.6	2.7	3.1	2.7
Sm_2O_3	1.4	3.2	3.6	4.2	3.4	3.6	3.6	3.4	4.1	3.8	3.8	1.4	1.5	2.3	2.0
Gd_2O_3	2.3	4.8	5.2	5.0	4.3	4.9	4.2	4.4	7.0	4.5	4.9	2.5	2.3	3.3	3.5
Dy_2O_3	2.5	4.3	4.6	4.5	2.9	3.6	3.6	4.1	4.8	3.6	3.8	2.5	2.1	3.8	3.2
Er_2O_3	2.8	2.6	2.3	2.7	2.1	2.5	1.9	2.5	2.6	2.6	2.5	2.2	1.7	2.3	2.5
Yb_2O_3	2.7	2.7	2.1	2.5	1.9	2.4	1.5	2.2	2.1	2.3	2.0	2.2	1.9	2.3	2.4
Y_2O_3	1.2	19.4	20.2	20.2	19.0	18.5	20.1	19.8	19.7	16.9	15.5	31.0	30.9	28.1	30.2
ThO_2	1.2	1.0	0.6	0.2	1.0	1.1	0.3	0.6	0.4	0.5	0.6	<0.1	<0.1	<0.1	<0.1
UO_2	0.3	0.3	0.3	<0.1	0.2	0.2	<0.1	0.2	0.2	0.2	0.4	<0.1	<0.1	<0.1	<0.1
CaO	0.4	3.3	2.2	1.2	2.8	2.8	3.6	1.9	1.9	2.0	2.2	2.7	3.1	2.0	2.3
FeO†	0.9	8.3	9.9	11.8	11.1	8.5	13.3	9.7	10.5	10.1	9.8	6.9	7.8	5.3	5.4
SiO_2	1.0	22.5	22.6	22.6	22.7	22.8	23.6	22.3	23.6	22.4	21.6	26.6	26.3	24.9	25.2
BeO‡		9.4	9.4	9.4	9.5	9.5	9.8	9.3	9.8	9.3	9.0	11.1	10.9	10.4	10.5
H_2O‡		1.3	0.9	0.4	0.6	1.3	0.2	0.9	0.9	0.8	0.8	2.3	2.0	2.4	2.4
Total		92.5	94.5	96.0	94.1	93.5	98.7	93.0	95.9	94.5	92.0	99.7	99.3	96.5	97.2
Formula proportions based on 10 O atoms															
La		0.03	0.03	0.03	0.03	0.03	0.03	0.03	0.02	0.04	0.05	0.04	0.04	0.04	0.03
Ce		0.11	0.11	0.13	0.14	0.13	0.15	0.14	0.06	0.18	0.19	0.10	0.11	0.12	0.09
Pr		0.03	0.04	0.05	0.04	0.04	0.05	0.04	0.03	0.06	0.05	0.02	0.02	0.03	0.03
Nd		0.13	0.17	0.16	0.18	0.18	0.17	0.18	0.15	0.23	0.23	0.07	0.07	0.09	0.08
Sm		0.10	0.11	0.13	0.10	0.11	0.11	0.10	0.12	0.12	0.12	0.04	0.04	0.06	0.06
Gd		0.14	0.15	0.15	0.13	0.14	0.12	0.13	0.20	0.13	0.15	0.06	0.06	0.09	0.09
Dy		0.12	0.13	0.13	0.08	0.10	0.10	0.12	0.13	0.11	0.12	0.06	0.05	0.10	0.08
Er		0.07	0.06	0.07	0.06	0.07	0.05	0.07	0.07	0.07	0.07	0.05	0.04	0.06	0.06
Yb		0.07	0.06	0.07	0.05	0.07	0.04	0.06	0.06	0.06	0.06	0.05	0.04	0.06	0.06
Y		0.92	0.96	0.96	0.90	0.87	0.91	0.95	0.91	0.81	0.77	1.26	1.27	1.21	1.28
Th		0.02	0.01	0.00	0.02	0.02	0.01	0.01	0.01	0.04	0.05	0.00	0.00	0.00	0.00
U		0.01	0.00	0.00	0.00	0.00	0.00	0.00	0.00	0.02	0.03	0.00	0.00	0.00	0.00
Ca		0.31	0.21	0.11	0.27	0.26	0.33	0.19	0.18	0.19	0.22	0.23	0.26	0.18	0.20
Fe		0.62	0.74	0.88	0.83	0.63	0.95	0.73	0.76	0.76	0.77	0.44	0.50	0.36	0.36
Si		2.01	2.01	2.02	2.02	2.02	2.02	2.01	2.05	2.02	2.01	2.04	2.03	2.01	2.01
Be		2.01	2.01	2.02	2.02	2.02	2.02	2.01	2.05	2.02	2.01	2.04	2.03	2.01	2.01
OH		0.77	0.54	0.25	0.36	0.76	0.12	0.55	0.52	0.50	0.48	1.15	1.02	1.30	1.29
Me	2.1	2.0	2.0	2.0	2.0	2.1	2.0	1.9	2.1	2.1	2.0	2.0	2.0	2.0	
Me/Si	1.0	1.0	1.0	1.0	1.0	1.0	1.0	1.0	1.0	1.0	1.0	1.0	1.0	1.0	
Y/Dy	7.4	7.2	7.4	10.9	8.4	9.2	8.1	6.8	7.7	6.7	20.6	24.0	12.3	15.6	

* Percentage standard deviation based on counting statistics.
† Total iron as FeO.
‡ Calculated as explained in the text.

Powder XRD diffraction analyses indicate a partial to complete metamict state for samples B1, B2, and B3. The other crystals possess metamict cores, but good diffraction patterns were obtained for the rims. Moreover, low totals for gadolinite minerals have been reported in previous studies such as Demartin et al. (1993) and Belolipetskii and Voloshin (1996). In the metamict state, the minerals present a disordered structure that facilitates the chemical mobility during alteration processes such as weathering. Because of these phenomena some crystals of the gadolinite-group minerals from Baveno and Cuasso al Monte could degenerate into a porous, amorphous assemblage of hydrated oxides of less mobile elements such as Fe. Indeed, in some deeply altered crystals from sample B3, which have a porous microstructure and contain hydroxides, the analyses (not reported in the tables) yield very low totals (91–92 wt%) and show a significant increase in their Fe content (up to 40 wt%, cf. Fig. 6).

Despite the observed metamict state, for much of the samples, the stoichiometric atomic ratios Me/Si (where Me indicates the sum of Y + REE + Ca + Th + U) is close to the throretical value of 1.0. The values of the Me/Si ratio also indicate a lack of extensive substitutions of B or Be for silicon. I addition, Me is always close to 2 indicating that Y, REE, Ca, Th, and U probably fill the W site. This site occupancy seems to eliminate the possibility that additional Ca is present in the X site, as in minasgeraisite, but a confirmation can be obtained only by means of a crystal structure analysis.

Figures 5a and 5b show chondrite-normalized rare earth elements (REE) patterns. The results indicate similar behavior for both the localities with the exception of Ce, which is slightly more enriched in most of the Baveno samples. The middle to heaby REE (Sm → Yb) are relatively unfractionated, and the light REE are steeply fractionated.

The analyses of the gadolinite-group minerals are shown in Figures 6 and 7 in terms of formula proportions Fe and Ca. These diagrams show a different distribution of compositions for Baveno compared with Cuasso al Monte. At Baveno, the analyses of samples B1 and B2 plot close to end-member gadolinite. Sample B3 shows compositions that range from end-member gadolinite to gadolinite with a moderate amount of the hingganite component. The crystals from miarolitic cavities, B4 and B5, display a large range of compositions from gadolinite to hingganite, with a high amount of the datolite component. The hingganite compositions have been found mainly in the rims of crystals. An analysis of a large omogeneous datolite crystal from a cavity from Baveno (not reported in Table 1 because of its stoichiometric comporition) plots close to the composition of datolite end-member. At Cuasso al Monte, datolite is absent and the Ca content is always low and relatively constant for all samples (≤0.50 apfu Ca). Gadolinite end-member compositions are not observed, and hingganite compositions are present in the rim of sample C3.

Referring to the scheme of Nickel and Grice (1998) gadolinites and hingganites from Baveno and Cuasso al Monte may be classified on the basis of the cation content in the W site. In the samples from Baveno, Y is the dominant cation. The core of sample B1 is gadolinite-(Y), with ΣREE prevailing over Y and with Ce dominant among the REE. The remaining por-

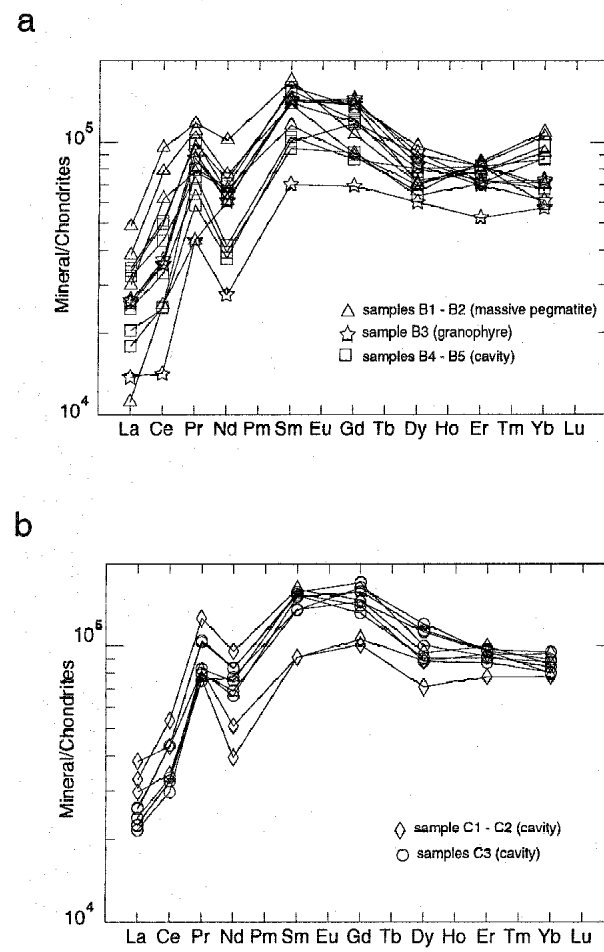

FIGURE 5. Chondrite-normalized REE patterns for gadolinite-group minerals from Baveno (a) and Cuasso al Monte (b). Chondrite values used for normalization after Nakamura (1974).

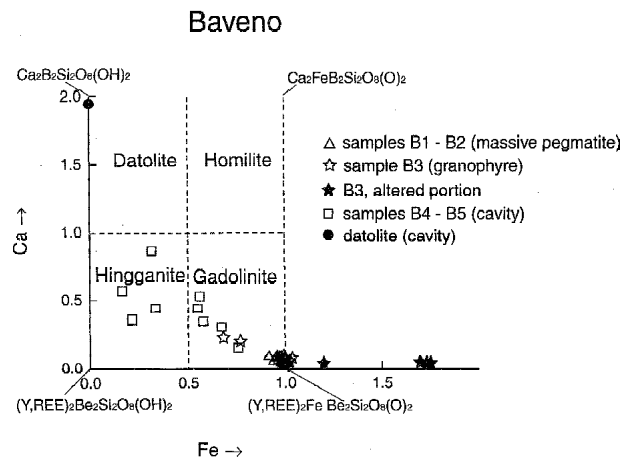

FIGURE 6. Compositional relationships of the gadolinite-group minerals occurring in the Baveno pluton.

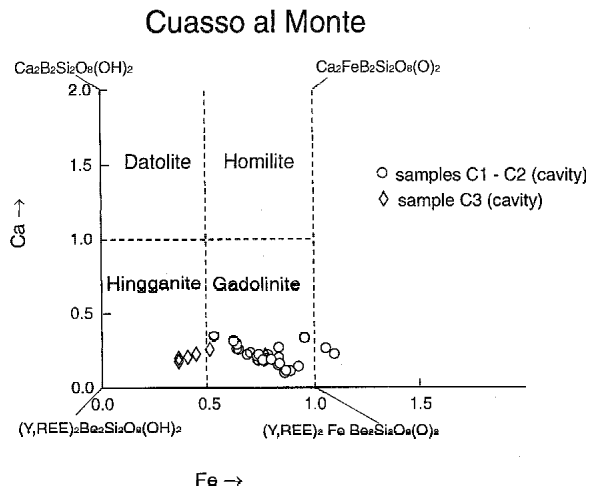

FIGURE 7. Compositional relationships of the gadolinite-group minerals occurring in the Cuasso al Monte granophyric granite.

tions of sample B1, samples B2 and B3, and the core of samples B4 and B5 are gadolinite-(Y), with Y prevailing over ΣREE. Hingganite-(Y), however, occurs in the rims of samples B4 and B5. Y is also the dominant element in gadolinites from Cuasso al Monte. However, the ΣREE prevail over Y, with Nd dominant, in the cores. In the remaining parts of the crystals, gadolinite-(Y) occurs with Y prevailing over ΣREE. In sample C3, hingganite-(Y) is present in the intermediate and peripheral zones of the crystal.

Figure 8 shows the Y/Dy-variation from core to rim of the studied crystals. In the samples from Baveno, an increase of the Y/Dy values is observed. In samples B4 and B5, a significant decrease followed by an increase is observed in the Y/Dy-ratio toward the rim. At Cuasso al Monte, the Y/Dy-ratios in sample C1 are relatively constant. Samples C2 and C3 show an oscillatory variation, with very high values of Y/Dy-ratios close to the rim of C3.

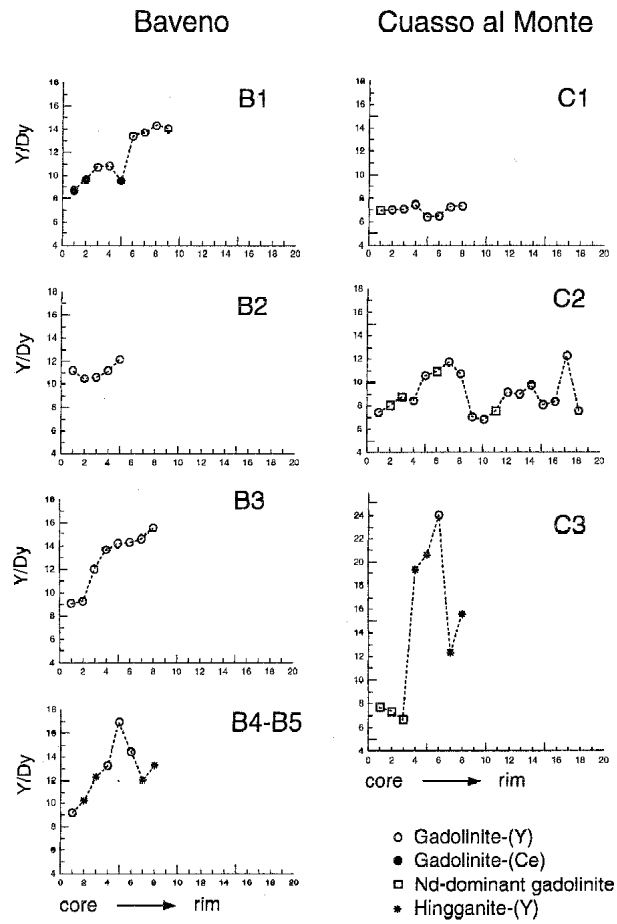

FIGURE 8. Y/Dy-ratio variations from core to rim of the studied crystals. The error, not reported, is in the range ±0.3–1.0.

DISCUSSION AND CONCLUSIONS

At Baveno, Ce-rich gadolinite-(Y) (with ΣREE >Y) and gadolinite-(Y) (with ΣREE <Y) formed during the early stages of crystallization of pegmatitic veins, where they are associated with feldspar, quartz, and siderophyllite. Based on experimental data on pegmatitic melts (London 1992), the occurrence of gadolinites between the peripheral graphic unit and the cavities indicates crystallization from a fluid-rich silicate-melt. Gadolinite-(Y) crystallized from a similar melt at more-evolved stages in pegmatites and in moderately evolved granophyric aplites. In the cavities, gadolinite-(Y) and a later hingganite-(Y), which contains a significant datolite component, crystallized from hydrothermal fluids together with many rare-element accessory phases. At the latest stages of cavity formation, datolite formed together with zeolite.

At Cuasso al Monte, gadolinite-group minerals were observed only in primitive to highly evolved cavities where they crystallized from either a residual fluid-rich melt or from hydrothermal fluids only. The most primitive gadolinite-composition, a Nd-rich gadolinite-(Y) (with ΣREE>Y), occurs in the cores of these crystals. In primitive cavities, Nd-rich gadolinite-(Y) (with ΣREE>Y) was followed by gadolinite-(Y) (with ΣREE<Y). In highly evolved cavities, gadolinite-(Y) with a high hingganite component and later hingganite-(Y) are present together with several rare-element phases.

The chemical differences observed between the most primitive gadolinites of Baveno and Cuasso al Monte (Ce-rich and Nd-rich, respectively) may reflect a different parental magma composition. In particular, the Ce content of gadolinites from Baveno could indicate contamination of source material with a supracrustal component (Henderson 1996).

The chemical differences between the "evolved" gadolinites from the two localities and, in particular, the absence of datolite and of a datolite component enrichment in hingganite at Cuasso al Monte, reflect a difference in the paragenesis and probably in the crystallization process. In particular, in contrast to Baveno, the crystallization in the strongly miarolitic granophyre of Cuasso al Monte occurred in open-system conditions preventing the formation of a zeolite (datolite-bearing) stage and generating a typical medium- to low-temperature hydrothermal mineral assemblage with quartz, fluorite, barite, sulfides, and carbonates.

At both localities, the complex fluctuations of the composi-

tion observed in the crystals in pockets with highly evolved paragenesis is in agreement with the observations of complex chemical zoning in hydrothermal RE minerals from other localities (Gieré 1996, and references therein). The Y/Dy-ratio variations (Fig. 8) indicate the existence of a mechanism capable of producing a significant change of this value during crystallization. The geochemical behavior of Y^{3+} and REE^{3+} is ordinarily explained on the basis of differences in the ionic radii linked to the phenomenon of lanthanide contraction. Consequently, the abundance ratio between Y and the REE having the most similar ionic radius should remain constant. The large range in Y/Dy values in the studied samples could be explained by considering the variations of the fluorine abundance in the hydrothermal fluids related to paragenetic and/or mixing effects. Indeed, the stability constants for fluoride complexes of Y are higher by a factor of two than those of the REE with the closest ionic radii (Gd, Tb, Dy) (Gramaccioli and Pezzotta 1999 and references therein; Gramaccioli et al., unpublished manuscript). This difference in the stability constants could reflect a difference in the behavior of these elements in fluids that is large enough to explain the observed variations in Y/Dy ratio.

ACKNOWLEDGMENTS

The authors are grateful to C.M. Gramaccioli for helpful discussion and continued encouragement, to F. Demartin for XRD analyses, and P. Gentile and C. Albertini for providing part of the studied samples. This work was financially supported by the National Research Council (C.N.R.), Centro di Studio per la Geodinamica alpina e quaternaria, and by the Museo di Storia Naturale of Milan. R. Gieré and K. Alstrup Jensen are thanked for detailed suggestions that helped improve the manuscript.

REFERENCES CITED

Bakos, F., Del Moro, A., and Visonà, D. (1990) The Hercynian volcano-plutonic association of Ganna (Lake Lugano, Central Southern Alps, Italy). European Journal of Mineralogy, 2, 373–383.

Belolipetskii, A.P. and Voloshin, A.V. (1996) Yttrium and rare earth element minerals of the Kola Peninsula, Russia. In A.P. Jones, F. Wall, and C.T. Williams, Eds., Rare Earth Minerals. Chemistry, origin and ore deposits, p. 311–326. Chapman & Hall, London.

Bonin, B. (1988) From orogenic to anorogenic environments: evidence from associated magmatic episodes. Schweizerische Mineralogische und Petrographische Mitteilungen, 68, 301–311.

Boriani, A., Caironi, V., Giobbi Origoni, E., and Vannucci, R. (1992) The Permian intrusive rocks of Serie dei Laghi (Western Southern Alps). Acta Vulcanologica, Marinelli Volume, 2, 73–86.

Boscardin, M., De Michele V., and Scaini G. (1970) Itinerari mineralogici della Lombardia, p. 124. Società Italiana di Scienze Naturali, Milano.

Černý, P. (1991) Rare-element Granitic Pegmatites. Part I: Anatomy and Internal Evolution of Pegmatite Deposits. Geoscience Canada, 18, 2, 49–67.

Demartin, F., Pilati, T., Diella, V., Gentile, P., and Gramaccioli, C.M. (1993) A crystal-chemical investigation of Alpine gadolinite. Canadian Mineralogist, 31, 127–136.

Fagnani, G. (1941) Nuovi ritrovamenti di gadolinite nel granito di Baveno. Natura. Società Italiana di Scienze Naturali, Milano, 40, 84.

Foord, E.E., Gaines, R.V., Crock, J.G., Simmons, W.B., and Barbosa, C.P. (1986) Minasgeraisite, a new member of the gadolinite group from Minas Gerais, American Mineralogist, 71, 603–607.

Gieré, R. (1996) Formation of rare earth minerals in hydrothermal system. In A.P. Jones, F. Wall, and C.T. Williams, Eds., Rare Earth Minerals. Chemistry, origin and ore deposits, p. 105–150. Chapman & Hall, London.

Gramaccioli, C.M. (1975) Minerali Alpini e Prealpini. Istituto Italiano Edizioni Atlas, Bergamo, p. 473.

Gramaccioli, C.M. and Pezzotta, F. (1999) Geochemistry of Yttrium with respect to the Rare-Earth elements in pegmatites. Memorie Società Italiana di Scienze Naturali, in press.

Grill, E. (1937) Titanite, allanite e gadolinite isotropa del granito di Baveno. Atti Società Italiana di Scienze Naturali, 76, 384–388.

Guastoni, A. and Pezzotta, F. (1999) I minerali del gruppo della gadolinite nelle località di Baveno e Cuasso al Monte. Rivista Mineralogica Italiana, in press.

Henderson, P. (1996) The rare earth elements: introduction and review. In A.P. Jones, F. Wall, and C.T. Williams, Eds., Rare Earth Minerals. Chemistry, origin and ore deposits, p. 1–20. Chapman & Hall, London.

Khomyakov, A.P. (1995) Mineralogy of Hyperagpaitic Alkaline Rocks (translated from the Russian by Khomyakov, P.A. and Rassadin B.V.) p. 223. Clarendon Press, Oxford.

Kipfer, A. (1983) Die mineralparagenesen der granophyre von Carona und Cuasso al Monte. Schweizer Strahler, Zurich, 6, 177–228.

Larsen, A.O. (1996) Rare earth minerals from the syenite pegmatites in the Oslo Region, Norway. In A.P. Jones, F. Wall, and C.T. Williams, Eds., Rare Earth Minerals. Chemistry, origin and ore deposits, p. 151–166. Chapman & Hall, London.

London, D. (1992) The application of experimental petrology to the genesis and crystallisation of granitic pegmatites. Canadian Mineralogist, 30, 499–540.

Mannucci, G, Diella, V., Gramaccioli, C.M., and Pilati, T. (1986) A comparative study of some pegmatitic and fissure monazite from the Alps. Canadian Mineralogist, 24, 469–474.

Mason, B. (1971) Ytterby, Sweden: a classic mineral locality. Mineralogical Record, 2, 136–138.

Nakamura, N. (1974) Determination of REE, Ba, Fe, Mg, Na, and K in carbonaceous and ordinary chondrite. Geochimica et Cosmochimica Acta, 38, 757–775.

Nickel, E.H. and Grice, J.D. (1998) The IMA Commission on New Minerals and Mineral Names: prodceudre and guidelines on mineral nomenclature, 1998. Canadian Mineralogist, 36, 913–926.

Pagliani, G. (1941) Gadolinite di Baveno. Rendiconti Società Italiana di Mineralogia e Petrologia, Milano, 1, 129–135.

Pinarelli, L., Boriani, A., and Conticelli, S. (1988) Rb-Sr geochronology of the Lower Permian plutonism in the Massiccio dei Laghi, Southern Alps (NW Italy). Rendiconti Società Italiana Mineralogia e Petrografia, 43, 411–428.

Wu, C., Yuan, Z., and Bai, G. (1996) Rare earth deposits in China. In A.P. Jones, F. Wall, and C.T. Williams, Eds., Rare Earth Minerals. Chemistry, origin and ore deposits, p. 281–310. Chapman & Hall, London.

MANUSCRIPT RECEIVED SEPTEMBER 9, 1998
MANUSCRIPT ACCEPTED JANUARY 4, 1999
PAPER HANDLED BY RODNEY C. EWING